Anaesth Crit Care Pain Med 40 (2021) 100852

Contents lists available at ScienceDirect

Anaesthesia Critical Care & Pain Medicine

journal homepage: www.elsevier.com

Review article

What are the echocardiographic findings of acute right ventricular strain that suggest pulmonary embolism?

Stephen Alerhand [a,*], Tina Sundaram [b], Michael Gottlieb [b]

[a] Department of Emergency Medicine, Rutgers New Jersey Medical School, 150 Bergen Street, Newark, NJ 07103, USA
[b] Department of Emergency Medicine, Rush University Medical Center, 1750 W. Harrison Street, Kellogg Suite 108, Chicago, IL 60612, USA

ARTICLE INFO

Article history:
Available online 26 March 2021

Keywords:
Point-of-care ultrasound
POCUS
Echocardiography
Pulmonary embolism
Right ventricular strain
Right ventricle
McConnell's sign
Tricuspid regurgitation
Pulmonary artery systolic pressure
Tricuspid annular plane systolic excursion
TAPSE
S'
Pulmonary artery mid-systolic notching
60/60 sign
Pulmonary artery acceleration time
Speckle tracking

ABSTRACT

Introduction: Pulmonary embolism (PE) is a potentially fatal disease encountered in the hospital setting. Prompt diagnosis and management can improve outcomes and survival. Unfortunately, a PE may be difficult to diagnose in a timely manner. Point-of-care ultrasound (POCUS) can assist in the evaluation for suspected PE by assessing for acute right ventricular strain. Physicians should thus be aware of these echocardiographic findings.
Objective: This manuscript will review ten echocardiographic findings of right ventricular strain that may suggest a diagnosis of PE. It will provide a description of each finding along with the associated pathophysiology. It will also summarize the literature for the diagnostic utility of echocardiography for this indication, while providing reference parameters where applicable. Along with labeled images and video clips, the review will then illustrate how to evaluate for each of the ten findings, while offering pearls and pitfalls in this bedside evaluation.
Discussion: The ten echocardiographic findings of right ventricular strain are: increased right ventricle: left ventricle size ratio, abnormal septal motion, McConnell's sign, tricuspid regurgitation, elevated pulmonary artery systolic pressure, decreased tricuspid annular plane systolic excursion, decreased S', pulmonary artery mid-systolic notching, 60/60 sign, and speckle tracking demonstrating decreased right ventricular free wall strain.
Conclusions: Physicians must recognize and understand the echocardiographic findings and associated pathophysiology of right ventricular strain. In the proper clinical context, these findings can point toward a diagnosis of PE and thereby lead to earlier initiation of directed management.
© 2021 Société française d'anesthésie et de réanimation (Sfar). Published by Elsevier Masson SAS. All rights reserved.

1. Introduction

Pulmonary embolism (PE) is a potentially fatal disease encountered in the hospital setting. Mortality rates for non-massive, sub-massive, and massive PEs are < 5%, 3–15%, and 25–50%, respectively [1]. Prompt diagnosis and management may improve outcomes and survival [2]. Unfortunately, PEs may be difficult to diagnose in a timely manner. In the proper clinical context, point-of-care ultrasound (POCUS) can assist in the evaluation for suspected PE by assessing for acute right ventricular strain. Sensitivities and specificities overall are driven by pre-test probability. For instance, POCUS is highly sensitive for large, centrally located PEs [3] and those with abnormal vital signs [4]. Physicians should thus recognize and appreciate the echocardiographic findings of acute right ventricular strain in the setting of a suspected PE.

This narrative review will describe ten individual echocardiographic findings manifested by right ventricular strain from a PE, detail the associated pathophysiology, offer evidence for echocardiography's diagnostic utility (among patients already being evaluated for PE), and provide reference parameters where applicable. The manuscript will then present labeled images and videos to provide succinct tutorials, while offering pearls and pitfalls for translation to the bedside evaluation.

2. Methods

The authors searched PubMed and Google Scholar for articles using a combination of the keywords "right ventricular strain", "right heart strain", "right ventricle", "echocardiography", "ultra-

* Corresponding author at: Department of Emergency Medicine, Rutgers New Jersey Medical School, 150 Bergen Street, Newark, NJ 07103, USA.
E-mail address: Stephen.Alerhand@gmail.com (S. Alerhand).

https://doi.org/10.1016/j.accpm.2021.100852
2352-5568/© 2021 Société française d'anesthésie et de réanimation (Sfar). Published by Elsevier Masson SAS. All rights reserved.

SHOUT
SHARE
IT

sound", "point-of-care ultrasound", "pulmonary embolism", and each of the echocardiographic findings listed as subheadings below. Authors included clinical guidelines, systematic reviews and meta-analyses, prospective studies, and retrospective studies. The literature search was restricted to studies published in English. Physicians with Clinical Ultrasound Fellowship training and experience in critical appraisal of the literature reviewed all of the articles and decided which ones to include for the review by consensus.

3. Discussion

3.1. Increased right ventricle: left ventricle size ratio

3.1.1. Description

The flow produced by the right ventricle (RV) generates a certain level of mean pressure based on the resistance of the pulmonary circulation. This pressure is much lower than that of the left ventricle (LV) pushing blood through the systemic circulation where there is higher resistance. A PE will cause an acute increase in the pulmonary vascular resistance (PVR) and right ventricular afterload. Since the right ventricular wall is thin and relatively compliant, this will lead to a rapid enlargement in RV size. Right ventricular enlargement portends poor outcomes such as in-hospital PE-related shock, need for cardiopulmonary resuscitation, and PE-related mortality [5–7]. A retrospective study found that patients with PE who had both right ventricular enlargement and elevated troponin had a higher 30-day mortality rate (38%) than patients with an elevated troponin alone (23%), with right ventricular dilation alone (9%), or with neither adverse prognostic marker (5%) [8].

A normal ratio of RV:LV size is 0.67:1 [9,10] (Video 1a) (Fig. 1a). The RV is considered to be mildly dilated if the RV:LV ratio is between 0.67:1 to 1:1, moderately dilated if between 1:1 and 1.5:1 (Video 1b) (Fig. 1b), and severely dilated if greater than 1.5:1 [9,10] (Video 1c) (Fig. 1c).

3.1.2. Evidence

A systematic review and meta-analysis (SRMA) showed that enlargement of the RV compared with the LV is 55% sensitive and 86% specific for PE [11]. When assessed only among studies performed by physicians, it was found to be 46% sensitive and 91% specific [11]. One of the studies evaluating emergency physicians in particular demonstrated a 96% interobserver agreement [12]. A prospective study of emergency physicians later found that when patients had a heart rate (HR) $\geq$ 100 beats per minute (bpm) and/or a systolic blood pressure (SBP) $<$ 90 mmHg, right ventricular dilation was 51% sensitive and 86% specific for PE [4]. When HR $\geq$ 110 bpm, right ventricular dilation was 57% sensitive and 84% specific with 89% interrater reliability. Interestingly, one study found that quantitation of right ventricular dimensions improved interreader agreement [13]. By this standard, the American Society of Echocardiography (ASE) and European Association of Cardiovascular Imaging (EACVI) state that a basal right ventricular diameter $>$ 41 mm and mid-level right ventricular diameter $>$ 35 mm suggest right ventricular dilation [10].

3.1.3. How to assess

1. Acquire an RV-focused apical-4-chamber (A4C) view [9].
   a. The RV can be imaged through various planes in the standard A4C view. Therefore, its areas and dimensions may vary widely in the same patient with relatively minor rotations in transducer position. For focused assessment of the RV, the largest basal right ventricular diameter should be displayed in order to capture the chamber's largest area [9].
2. The relative ventricular sizes can be assessed qualitatively (Video 1) or by quantitative measurement of the mid-free wall to the septum at end-diastole, when the chambers are at their largest (Fig. 1).

3.1.4. Pearls and pitfalls

Evaluation of right ventricular free wall thickness can help determine whether right ventricular dilation is due to an acute (*e.g.*, PE) or chronic etiology. This measurement should be performed in the subxiphoid (SX) view, with the right ventricular free wall oriented horizontally on the screen and the caliper measurement oriented perpendicularly (Fig. 2). This will take advantage of the ultrasound machine's superior axial resolution. The measurement should be made below the tricuspid annulus (*i.e.*, toward the right ventricular apex) at a distance approximating the length of a fully open anterior tricuspid leaflet parallel to the right ventricular free wall [10]. Trabeculations, papillary muscles, and epicardial fat should be excluded from the endocardial border [9]. ASE guidelines state that right ventricular wall thickness $>$5 mm measured at end-diastole (using either B-mode or M-mode) is suggestive of chronic right ventricular hypertrophy [9,14,15] (Fig. 2b).

3.2. Abnormal septal motion

3.2.1. Description

The filling pressure of the LV is normally greater than that of the RV, which pushes the interventricular septum toward the center of the RV (Video 2a). Abnormal septal motion seen in PE, or septal dyskinesia, refers to flattening or bowing of the interventricular septum away from the center of the RV and toward the center of the LV [7,9,12,16–23] (Video 2b) (Fig. 3). This finding reflective of right ventricular pressure overload can be visualized both at end-diastole and end-systole. During diastole, this occurs due to acute dilation of the RV with constriction by the pericardium. During systole, this finding occurs due to a reduction of the normal pressure gradient between the LV and RV from the decrease in left ventricular preload and increase in right ventricular pressure load

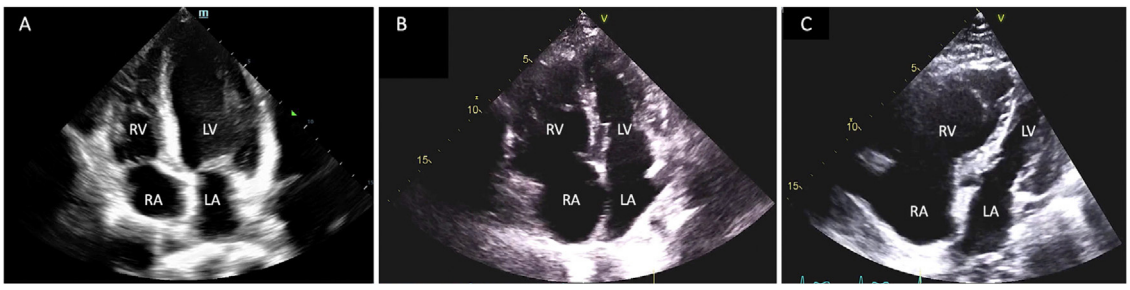

Fig. 1. Assessment of right ventricular size in the apical 4-chamber view: a) Normal right ventricle b) Moderately dilated right ventricle c) Severely dilated right ventricle.

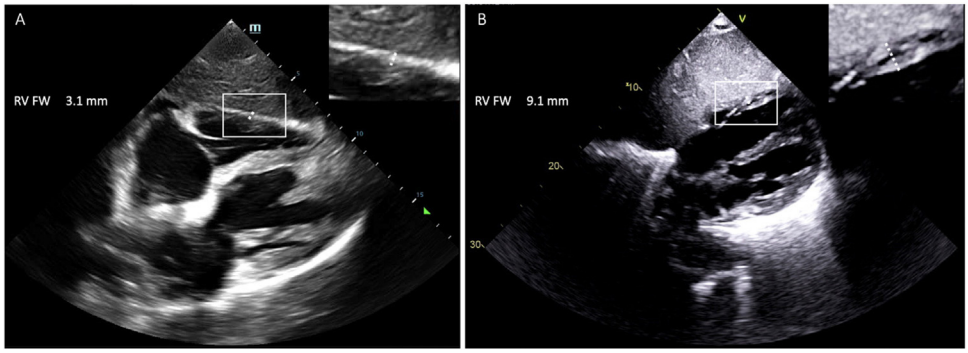

Fig. 2. Measurement of right ventricular free wall thickness at end-diastole in the subxiphoid view: a) Normal wall thickness b) Increased wall thickness > 5 mm.

[9,19]. Moreover, when right ventricular systole is overloaded, its contraction is prolonged. Consequently, the RV continues to contract after left ventricular systole has ended, at which point right ventricular pressure is greater than left. These dynamics between the two ventricles illustrate the principle of ventricular interdependence.

3.2.2. Evidence

In an SRMA, abnormal septal motion showed 26% sensitivity and 95% specificity for PE [11]. When assessed only among studies performed by physicians, sensitivity was 28% and specificity was 96% [11], with interobserver agreement reaching up to 100% [12]. A prospective study of emergency physicians in particular found that with a HR $\geq$ 100 bpm and/or an SBP $<$ 90 mmHg, septal flattening was 43% sensitive and 93% specific for PE [4]. When the HR $\geq$ 110 bpm, septal flattening was 47% sensitive and specificity remained 93%. Abnormal septal motion appears most often in patients with large clot burden or hemodynamic instability requiring intensive care [12].

3.2.3. How to assess

1. Acquire a parasternal short-axis (PSAX) view at the level of the papillary muscles.
2. A D-shaped septum will be seen with interventricular septal flattening or reversal of septal curvature toward the center of the LV (Video 2b) (Fig. 3).

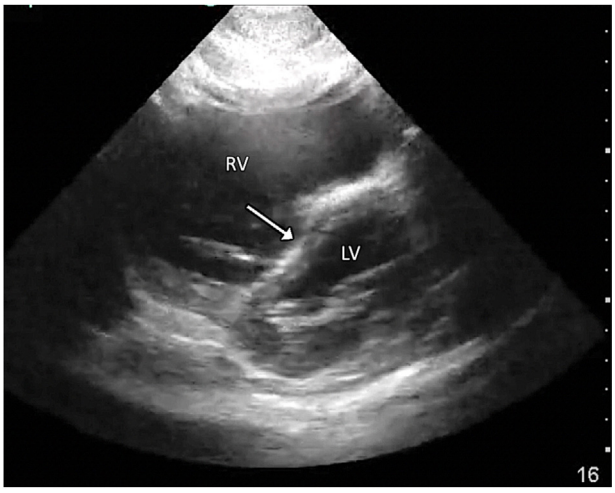

Fig. 3. Abnormal septal motion (D-shaped interventricular septum) in the parasternal short-axis view. The arrow indicates the direction of septal movement toward the center of the left ventricle.

a. Though this finding can be seen qualitatively throughout the cardiac cycle, the most marked distortion can be seen at end-systole, when the change in pressure gradient between RV and LV is maximal [9,24,25].

3.2.4. Pearls and pitfalls

Patients with a history of pulmonary hypertension may also have paradoxical septal motion due to right ventricular dilation and elevated pulmonary pressures [22]. Additionally, in patients with tricuspid regurgitation, an increase in right ventricular volume can lead to abnormal interventricular septum shift at end-diastole [9]. Lastly, in patients with PE who have concurrent left ventricular dysfunction, it has been theorized that normal septal motion may be visualized due to the balanced dilation of both ventricles [26].

3.3. McConnell's sign

3.3.1. Description

First described in 1996, McConnell's sign refers to diffuse hypokinesis of the RV with apical sparing, such that only the apex contracts well during systole [27] (Video 3) (Fig. 4). The original authors noted that apical sparing was useful to differentiate right ventricular strain due to an acute PE from that associated with more chronic etiologies (*e.g.*, pulmonary hypertension) [27].

Several mechanisms have been proposed to explain these findings. One explanation is that tethering of the right ventricular apex to the LV allows the right ventricular apex to be pulled inward

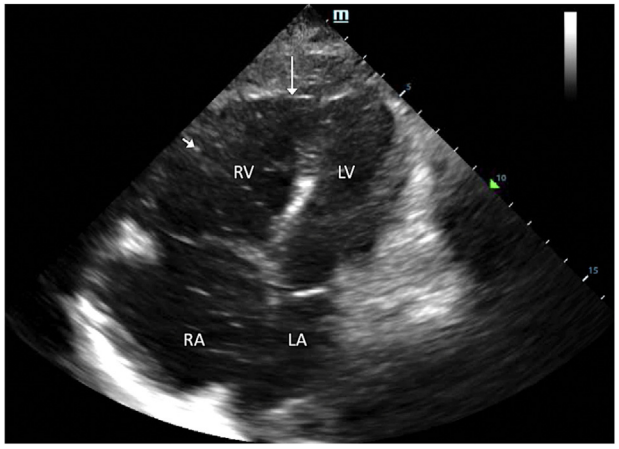

Fig. 4. McConnell's sign. The long arrow indicates normal apical systolic contraction (*i.e.*, apical sparing). The short arrow indicates right ventricular free wall hypokinesis.

by the hyperdynamic LV [27]. A second explanation is that the RV assumes a more spherical shape to equalize regional wall stress, aimed at counteracting the acute increase in afterload [27–29]. This leads to greater outward bulging of the mid-right ventricular free wall relative to the apex, giving the appearance of apical sparing [27]. By contrast, chronic right ventricular strain from pulmonary hypertension would lead to right ventricular hypertrophy, which may limit those tethering effects and shape changes [27,30]. Finally, the increased wall stress ($\propto$ ventricular pressure x radius/[2 x wall thickness]) from the acute pressure change may lead to localized ischemia of the right ventricular free wall (perfused by the right coronary artery), resulting in hypokinesis [27]. The apex, in contrast, is perfused by both the right coronary and left anterior descending arteries.

3.3.2. Evidence

The original study by McConnell reported 77% sensitivity and 94% specificity for PE [27]. However, a subsequent SRMA found McConnell's sign to be 22% sensitive and 97% specific for PE, with 19% sensitivity and 98% specificity when performed by physicians only [11]. A retrospective study found that McConnell's sign was 52% sensitive and 97% specific among patients with either massive or sub-massive PE [31]. In POCUS scans performed by emergency physicians, another study found that for patients with a HR $\geq$ 100 bpm and/or an SBP $<$ 90 mmHg, McConnell's sign was 35% sensitive and 99% specific for PE [4]. When the HR $>$ 110 bpm, McConnell's sign showed 36% sensitivity and 100% specificity. Interobserver agreement has ranged from 87 to 92% [27,32,33] with interobserver reliability having a kappa of 0.70 [34].

3.3.3. How to assess

1. Acquire an RV-focused A4C view.
2. Qualitatively assess for hypokinesis of the right ventricular free wall compared with normal apical systolic contraction (Video 3) (Fig. 4).

3.3.4. Pearls and pitfalls

Though not typically used, a quantitative assessment for McConnell's sign may also be performed. The original study found that the average free wall inward movement in PE was 0.2 mm, compared to an average apical movement of 5.7 mm [27]. Furthermore, though evidence suggests McConnell's sign is specific for PE, this finding may also be caused by right ventricular infarction [32,35,36].

3.4. Tricuspid regurgitation

3.4.1. Description

Tricuspid regurgitation (TR) occurs with PE due to dilation of the RV. As the thin, compliant right ventricular free wall balloons outward in the setting of increased PVR, the tricuspid valve annulus dilates. This leads to decreased coaptation of the tricuspid leaflets, with resultant regurgitation of flow through the tricuspid valve (Video 4) (Fig. 5). The maximum tricuspid regurgitation velocity (TRV_{max}) can be used as an indicator for severity of right ventricular strain.

ASE guidelines posit that TR_{max} velocity $>$ 2.8–2.9 m/s, which corresponds to a pulmonary artery systolic pressure (PASP) of approximately 36 mmHg (assuming right atrial pressure 3−5 mmHg), indicates elevated right ventricular systolic and pulmonary artery pressure (PAP) [9,37]. This is supported by various studies [16,20,37–41].

3.4.2. Evidence

An SRMA reported 40% sensitivity and 83% specificity of TR for PE, with 46% sensitivity and 87% specificity in physician-performed studies [11]. A retrospective study involving 2,139 patients found 90% agreement and a kappa of 0.85 between observers that were asked to classify TR as mild, moderate, or severe [41].

3.4.3. How to assess

1. TR can be assessed in the A4C, PSAX (preferably at the level of the aortic valve), or right ventricular inflow views using color Doppler (Video 4a,b,c) (Fig. 5a,b,c).
   a. These views orient blood flow roughly parallel to the transducer's emitted sound waves and thus obtain the maximal shift in Doppler frequency.
   b. To achieve the highest frame rate, minimize the size of the color Doppler box to encompass only the tricuspid valve and right atrium (RA), and adjust the study depth to the minimum required.
2. If a regurgitant jet is seen, place the continuous wave Doppler beam over the center of the jet, oriented parallel to the direction of blood flow.
3. By pressing the continuous wave Doppler button again, the TRV appears as a downward deflection on the y-axis. Bring the cursor over the well-defined velocity peak to obtain the TRV_{max}.
4. Among the A4C, PSAX, and right ventricular inflow views, use the highest obtainable TRV_{max} (Fig. 6a,b,c).

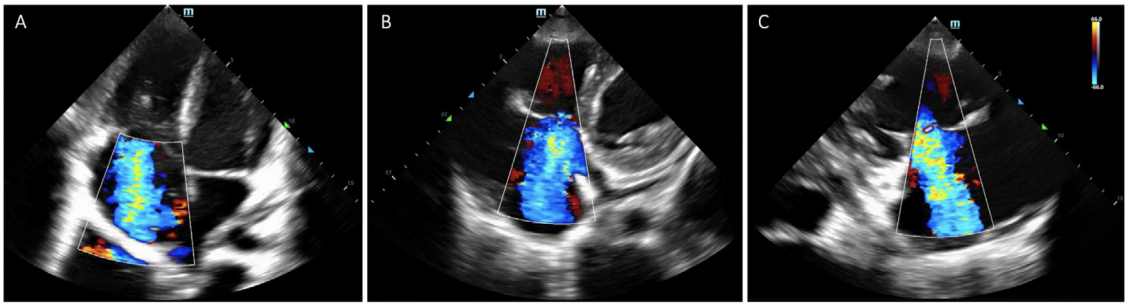

Fig. 5. Evaluation for tricuspid regurgitation: a) Apical 4-chamber view b) Parasternal short-axis view c) Right ventricular inflow view. These jets appear to represent severe tricuspid regurgitation. In all three views, the large regurgitation jets have vena contracta $>$ 7 mm, reflecting a large cross-sectional area of the blood column leaving the regurgitant orifice. All three jets also reach the posterior wall of the right atrium. In addition, the Coanda effect describes how eccentric jets may appear smaller than central jets of equal or lower severity, as the ventricular wall absorbs some of the eccentric jets' energy. Yet, the slightly eccentric jet in b) nevertheless occupies $>$ 50% of the right atrium area.

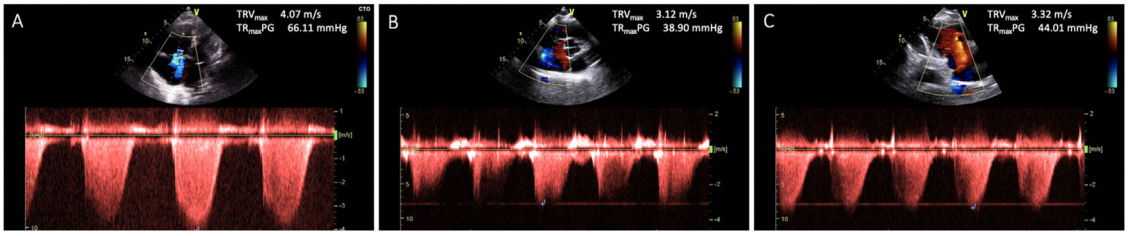

Fig. 6. Measurement of tricuspid regurgitation maximal velocity using continuous wave Doppler: a) Apical 4-chamber view b) Parasternal short-axis view c) Right ventricular inflow view. All three waveforms demonstrate a $TRV_{max} > 2.8–2.9$ m/s and high-density appearance that suggest high severity. The tricuspid regurgitation waveform profile is normally parabolic. When severe, the waveform becomes more triangular-shaped. First, there is early peaking of the velocity waveform. Next, with rapid pressure equalization of the right ventricle and right atrium, there is rapid deceleration of the Doppler tracing ("V" wave cutoff sign) like that seen in b). Also, the right atrium may be enlarged when the tricuspid regurgitation is chronic, like in a), which also has a tricuspid regurgitation pressure gradient > 60 mmHg (see Section 3.9).

3.4.4. Pearls and pitfalls

The measurement of TRV based on continuous wave Doppler can be unreliable and difficult to obtain [39]. Between 25–40% of patients may not demonstrate an adequate TR Doppler signal to determine PASP [41–43]. Additionally, TRV_{max} is non-diagnostic of acute right ventricular strain in cases of chronic right ventricular pressure overload, which is suggested by right ventricular free wall hypertrophy (thickness > 5 mm) [9]. In such cases, it is the chronic pressure overload that leads to dilation of the tricuspid valve annulus with resultant TR.

3.5. Elevated pulmonary artery systolic pressure

3.5.1. Description

Evaluation of pulmonary hypertension in PE uses the PASP as a marker of increased PVR. The PASP can be estimated using the simplified Bernoulli equation: pressure gradient between the RV and RA ($\Delta P_{RV\text{-}RA}$) = 4 x TRV_{max}^2. This value is then added to the mean right atrial pressure (RAP), acquired through assessment of the inferior vena cava (IVC) [9,44]. This method assumes no significant right ventricular outflow tract (RVOT) obstruction, or gradient across the pulmonic valve or RVOT, such that right ventricular systolic pressure equals PASP. One prospective study found close correlation (r = 0.97) between the PASP obtained using the TR Doppler gradient and that measured by cardiac catheterization [45].

Some studies suggest that a PASP > 30 mmHg in the absence of chronic pulmonary hypertension can be considered a sign of right ventricular strain and dysfunction [7,17,46]. ASE guidelines state that if the PASP is > 35–40 mmHg, stronger scrutiny may be warranted to determine if pulmonary hypertension is present [9]. It thus seems reasonable to posit a relative cut-off of > 35 mmHg in the setting of suspected or diagnosed PE. Of note, PASP has not been found to correlate significantly with in-hospital mortality rate in patients with PE [7].

The IVC diameter and presence or absence of inspiratory collapse can be used to estimate RAP [47]. As RAP increases, there is reduced inflow from the IVC to the RA. Therefore, the IVC remains dilated and does not collapse with inspiration (*i.e.*, negative intrathoracic pressure in the spontaneously breathing patient).

3.5.2. Evidence

An SRMA reported that elevated PASP found using echocardiography carries 44% sensitivity and 84% specificity for PE [11]. In studies evaluating physician-performed scans, there was 65% sensitivity and 74% specificity.

For the IVC evaluation, a review of the literature found that most studies demonstrated moderate-strength correlations between IVC diameter and RAP [48]. One study found that the use of IVC diameter to estimate RAP performed well for either low or high RAP, but less well for intermediate values [49]. Given the substantial heterogeneity in measurement techniques and patient populations, an overall correlation value is difficult to determine.

Of note, the IVC is commonly dilated and may not collapse in patients receiving mechanical ventilation (*i.e.*, positive-pressure ventilation with positive intrathoracic pressure). Therefore, caution should be used in such cases to estimate RAP [9,50–52]. Nevertheless, a prospective study of 49 mechanically ventilated patients found that an IVC diameter ≤ 1.2 cm appears accurate in identifying patients with RAP < 10 mmHg [52].

One prospective study showed that IVC measurement in B-mode by three experienced emergency physician sonographers had an intraclass correlation coefficient (ICC) of 86% [53]. Another prospective study found an ICC of only 60% among emergency physicians for visually estimating IVC collapse [54]. The ICC for the maximum and minimum IVC diameters using M-mode was 81% and 77%, respectively. When evaluating emergency medicine residents, another study found that measurements of maximum and minimum IVC diameters showed kappa of 56% and 60%, respectively, with higher interrater reliability for patients with deep or superficially located IVCs compared to moderate-depth IVC locations [55]. For pediatric emergency physicians (one novice in POCUS and one experienced), the interreviewer agreement for IVC collapse showed a kappa of 93% [56].

3.5.3. How to assess

1. To estimate $\Delta P_{RV\text{-}RA}$, the TRV_{max} obtained as described previously (Section 3.4.3) (Fig. 6) is entered into the simplified Bernoulli equation (4 x TRV_{max}^2).
2. Next, to estimate RAP, acquire the IVC at end-expiration in the SX view, with the IVC and RA displayed in long-axis.
   a. Measure the IVC diameter just proximal to the junction of the hepatic veins (about 0.5–3.0 cm proximal to the RA), perpendicularly to the length of the IVC to avoid overestimation [57–59].
      i. The patient should lie supine, because IVC diameter is larger in the right lateral decubitus position and smaller in the left lateral decubitus position [60].
   b. ASE guidelines recommend the following methodology to estimate RAP [9]:
      i. An IVC diameter ≤ 2.1 cm that collapses > 50% with a patient sniff (*i.e.* thin and collapsible) suggests a normal RAP of 3 mmHg (range 0–5 mmHg) (Video 5a).
      ii. An IVC diameter > 2.1 cm that collapses < 50% with a patient sniff (dilated and non-collapsible) suggests a high RAP of 15 mmHg (range 10–20 mmHg) (Video 5c).
      iii. When the IVC diameter and inspiratory collapse do not fit these parameters, an intermediate value of 8 mmHg (range 5–10 mmHg) may be assigned (Video 5b).

1. The following indices can be used to upgrade the RAP to 15 mmHg in indeterminate cases: a dilated RA, an interatrial septum bulging into the left atrium throughout the cardiac cycle, a restrictive right-sided diastolic filling pattern, a tricuspid E/e' ratio > 6, and diastolic flow predominance in the hepatic veins.

iv. If the patient is unable to perform a sniff, an IVC collapsing < 20% with quiet inspiration suggests an elevated RAP.

3. PASP = ΔP_{RV-RA} + RAP

3.5.4. Pearls and pitfalls

From a clinical perspective, a normal PASP in the setting of right ventricular dilation should raise concern for right ventricular infarction, and not necessarily acute PE. From a technical perspective, the same caveats and precautions previously described apply for obtaining TRV_{max} (see Section 3.4.4). Additionally, in about 50% of cases, there may be a discrepancy > 10 mmHg compared with invasive measurements [41,42,61]. At higher PAP, in particular, the Doppler technique may not be as accurate [61]. In these patients with very severe TR, the Doppler envelope may cut off due to early equalization of RV and RA pressures, and the simplified Bernoulli equation will thus underestimate the RV-RA gradient. Furthermore, PASP cannot be calculated if there is laminar TR flow across a wide-open tricuspid annulus, when the right side of the heart essentially acts as a single chamber during systole. The modified Bernoulli equation is valid only for narrow orifices with turbulent flow, and not when the inertial component of the Bernoulli equation must be incorporated. Lastly, when measuring the IVC during a sniff, the transducer may be at risk of moving to a different plane than the long axis of the IVC [9]. To guard against incorrect measurements, this diameter should be compared to that taken during quiet breathing.

3.6. Decreased tricuspid annular plane systolic excursion

3.6.1. Description

Tricuspid annular plane systolic excursion (TAPSE) is an easily performed, reproducible quantitative assessment that reflects the longitudinal contraction of the RV [62–64]. In the RV-focused A4C view, this one-dimensional measure of right ventricular systolic function is obtained in M-mode by measuring the vertical displacement of the lateral tricuspid annulus from the end of diastole to the end of systole (Fig. 7). This longitudinal contraction generated by the RV's deep subendocardial fibers constitutes 80% of the RV's cardiac output [14,65]. The greater the descent of the base toward the apex in systole (*i.e.*, toward the top of the screen), the better the right ventricular systolic function. TAPSE can reliably assess right ventricular dysfunction and RV ejection fraction (RVEF) as correlated with magnetic resonance imaging (MRI), right heart angiography, radionucleotide studies, fractional area change, and biplane Simpson's method [66–70]. Furthermore, as a prognostic tool, a decreased TAPSE in PE is independently predictive of 30-day mortality [64,71–74].

ASE guidelines posited < 16 mm as a cut-off value for abnormal right ventricular systolic dysfunction [9], though the ASE and EACVI later revised that cut-off to < 17 mm [10]. The latter guidelines reported a mean normal TAPSE 24 ± 3.5 mm [10].

3.6.2. Evidence

TAPSE appears to be decreased in patients with acute PE *versus* those without PE (15–19.5 mm *versus* 20–26 mm) [33,75,76]. Studies have used varying cut-off markers of TAPSE to determine sensitivities and specificities, which improve when tachycardia or hypotension are present [4,77]. A prospective study found that for emergency physicians evaluating patients with HR ≥ 100 bpm and/or SBP < 90 mmHg, a TAPSE cut-off of 20 mm showed 88% sensitivity and 73% specificity for PE, whereas a TAPSE cut-off of 17 mm showed 66% sensitivity and 85% specificity [4]. When HR > 110 bpm, a TAPSE cut-off of 20 mm showed 93% sensitivity and 73% specificity, whereas a TAPSE cut-off of 17 mm showed 77% sensitivity and 88% specificity [4].

One study assessing interobserver variability among cardiologists demonstrated an ICC of 0.85 and a kappa of 0.86 for an abnormal TAPSE [34]. Another study found that TAPSE was similarly reproduced by emergency physicians with an ICC of 0.87 and a kappa of 0.94 [77]. The latter author group found that even without a clearly defined quantitative value, emergency physicians with echocardiography training could qualitatively determine TAPSE as normal or abnormal with a kappa of 0.94 [77].

3.6.3. How to assess

1. Acquire an RV-focused A4C view.
   a. The four chambers should be visualized at their longest cross-section. This can be achieved by placing the transducer at the most inferior rib space feasible to acquire the A4C view, thereby aiming the ultrasound beam through the heart's true apex. This will prevent foreshortening of the RV with resultant underestimation of the longitudinal excursion of the lateral tricuspid annulus.
2. Place the M-mode beam over the lateral tricuspid annulus.

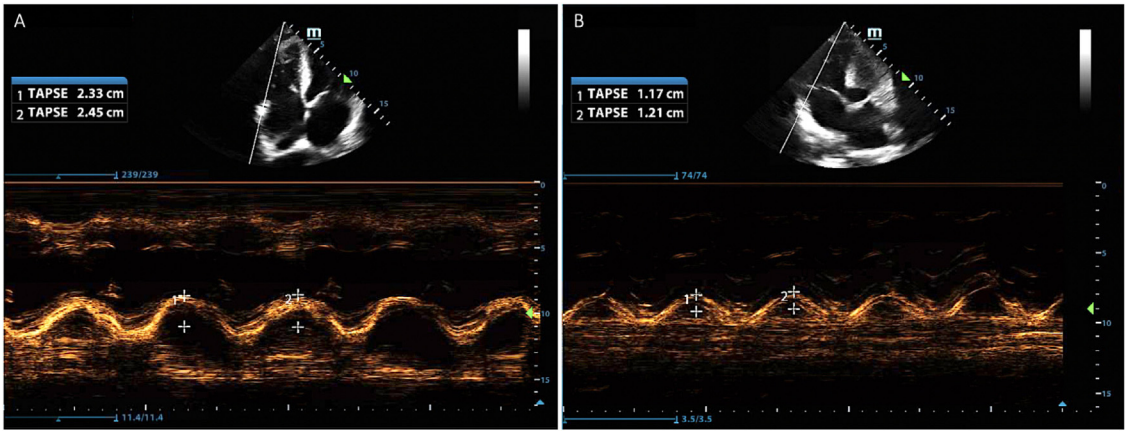

Fig. 7. Assessment of tricuspid annular plane systolic excursion: a) Normal b) Abnormal < 17 mm.

a. Align the beam parallel to the motion of the lateral tricuspid annulus towards the apex, in order to avoid underestimation of vertical displacement.
b. Consider decreasing the depth and gain in order to improve image resolution (*i.e.*, increase frame rate) and decrease artifact, respectively.

3. By pressing the M-mode button again, movement of the lateral tricuspid annulus appears on the y-axis. Measure from the top of the hyperechoic lateral tricuspid annulus signal in systole to the top of the hyperechoic annulus signal in diastole.
   a. Calculate the average of 3–4 consecutive cardiac cycles. Differentiate between normal (Fig. 7a) and abnormal (Fig. 7b).

3.6.4. Pearls and pitfalls

TAPSE measures the excursion of the lateral tricuspid annulus in only one (*i.e.*, longitudinal) dimension. It does not incorporate the contributions to RVEF from either the right ventricular free wall or interventricular septum. Thus, in cases of regional wall motion variation, TAPSE may not accurately reflect global right ventricular systolic function. In addition, poor right ventricular systolic function may have a normal TAPSE if a hyperdynamic LV is pulling strongly upon the RV.

3.7. Decreased S'

3.7.1. Description

S' refers to the systolic excursion velocity of the right ventricular basal free wall as it contracts longitudinally from base to apex [9] (Fig. 8). As with TAPSE, this measurement reflects the longitudinal contraction that constitutes 80% of the RV's cardiac output [14,65]. S' has been found to correlate well with RVEF based on MRI [78–81] and radionucleotide studies [66,82,83]. It also appears to be independent of patient age [84,85]. Studies have determined a normal S' to be $>$ 13−15 cm/s [80,83,85], with ASE and EACVI guidelines reporting a mean normal S' $>14.1 \pm 2.3$ cm/s [10].

Studies vary on the designations of right ventricular dysfunction (*e.g.* mild, moderate, and severe) by RVEF, as well as on the average S' values for each designation [66,79,80]. ASE guidelines posited that an S' $<$ 10 cm/s indicates right ventricular systolic dysfunction [9], thoughthe ASE and EACVI later revised this cut-off to $<$ 9.5 cm/s [10]. Of note, when the RVEF is below 40%, S' may remain almost constant around 9−10 cm/s [86].

3.7.2. Evidence

Sensitivities and specificities of S' for right ventricular dysfunction vary based on the cut-off values of S' used in those studies. Taken together, an S' cut-off value $<$ 11−12 cm/s can predict RVEF $<$ 45–50% with 74–90% sensitivity and 68–85% specificity [79–82]. An S' cut-off $<$ 9 cm/s can identify RVEF $<$ 30% with 82–83% sensitivity and 68–86% specificity [79,81]. Studies have demonstrated 3–15% intraobserver variability and 4–13% interobserver variability [80,82,83,85,87].

3.7.3. How to assess

1. Acquire an RV-focused A4C view.
2. Place the tissue Doppler sampling gate approximately 1 cm toward the apex from the lateral tricuspid annulus. This placement will ensure measurement of the ventricular (*versus* atrial) velocity.
   a. Align the beam parallel to the motion of the free wall towards the apex, in order to avoid underestimating the tissue velocity.
3. By pressing the tissue Doppler button again, the velocity of the basal free wall appears as a positive deflection on the y-axis during systole. Obtain the peak velocity by bringing the cursor to the peak of the waveform. Differentiate normal (Fig. 8a) from abnormal (Fig. 8b).

3.7.4. Pearls and pitfalls

Since the determination of S' comes from the longitudinal movement of roughly the same region (*i.e.*, the basal free wall) as TAPSE (*i.e.*, the lateral tricuspid annulus), the two values should roughly correlate in terms of being normal or abnormal. In addition, similar to TAPSE, the longitudinal measurement of S' does not incorporate the contributions to RVEF from either the right ventricular free wall or interventricular septum. Thus, in the setting of regional wall motion abnormalities, S' may not represent global right ventricular function. Of note, S' may also be reduced in patients with posterior myocardial infarction and chronic pulmonary hypertension [82].

3.8. Pulmonary artery mid-systolic notching

3.8.1. Description

When assessing Doppler flow of the pulmonary artery in patients without pulmonary disease, the waveform will typically appear like a "dome" due to the steady rise in PAP during systole [88] (Fig. 9a). However, when pulmonary hypertension is present, the flow will demonstrate a transient decrease in velocity during the pulmonary arterial systolic flow cycle, resulting in the appearance of biphasic flow (Fig. 9b). This is referred to as pulmonary artery mid-systolic notching [88–93]. This finding has been hypothesized to be caused by impedance of flow against elevated PAP [92,94,95], in that the reflected pressure waves return

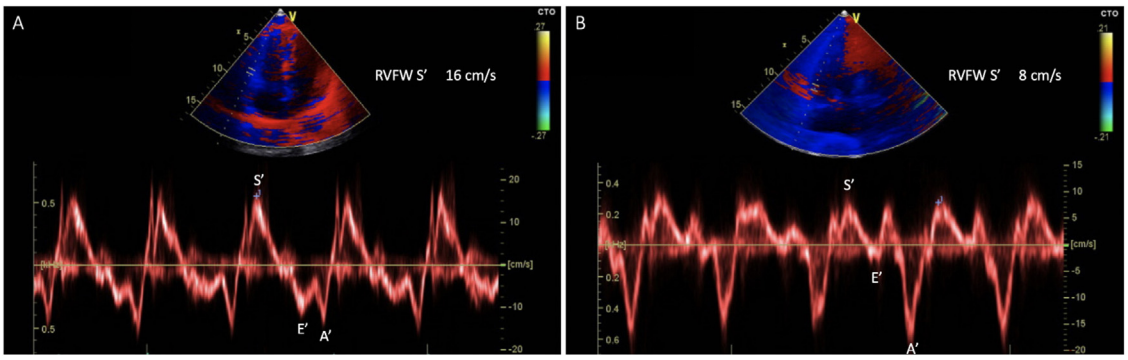

Fig. 8. Assessment of S': a) Normal b) Abnormal $<$ 9.5 cm/s.

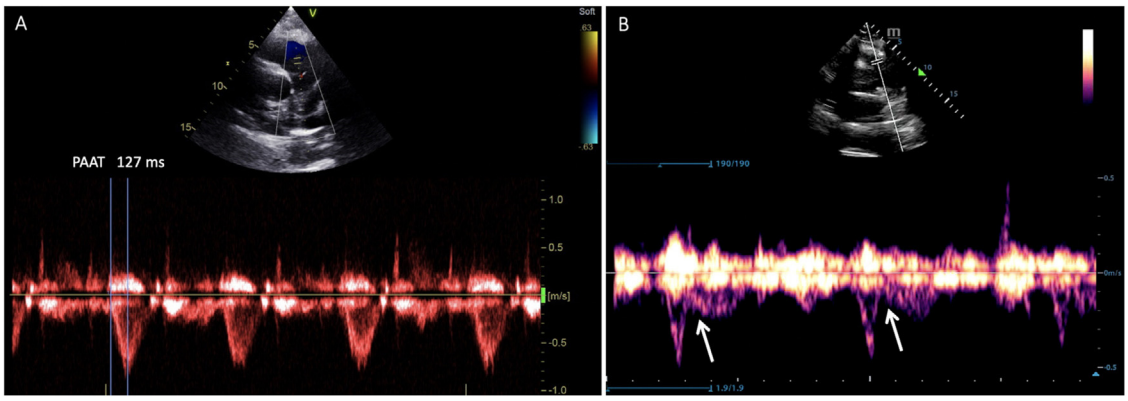

Fig. 9. Assessment of the pulmonary artery systolic ejection velocity waveform: a) Normal pulmonary artery acceleration waveform (“dome” pattern) b) Pulmonary artery early-systolic notching (“spike and dome” pattern).

prematurely due to their faster propagation in the non-compliant pulmonary vessels [96]. This impedance, which may be caused by a proximal arterial thrombus, causes transient reversal of the gradient between the pulmonary artery and RVOT.

One study found that the systolic flow velocity curve could be recorded in > 97% of patients [97]. Another study found that mid-systolic notching demonstrated 71% sensitivity and 96% specificity for increased PVR in patients with pulmonary hypertension [95]. A later study found that patients with a shorter time to mid-systolic notching (defined as a deceleration time < 120 ms) had more severe pulmonary disease and higher likelihood of all-cause mortality over three years [98].

3.8.2. Evidence

Pulmonary artery mid-systolic notching has been used to assess for increased PAP in the context of PE. One study found that mid-systolic notching was present in 100% of chronic PEs and 96% of acute PEs [99]. The patients with acute PE had a systolic flow velocity acceleration time (*i.e.*, time to peak velocity of the RVOT envelope) of 56 ± 15 ms and a time to maximum mid-systolic deceleration (*i.e.*, at the notch) of 105 ± 16 ms [99]. Another author group described the appearance of a “spike and dome” pattern from early-systolic notching, in which a narrow peaked initial waveform (*i.e.*, the spike) with early deceleration of the RVOT envelope (*i.e.*, toward the notch) was followed by a second Doppler waveform (*i.e.*, the dome) with a more curvilinear shape [31] (Fig. 9b). These authors found that early-systolic notching (within the initial 50% of the systolic ejection period) was 92% sensitive and 99% specific for massive or sub-massive PEs, *versus* only 2% sensitive for subsegmental PEs, with 97% interobserver agreement and a kappa of 0.93 [31]. Among patients with massive or sub-massive PE, systolic notching was predominantly early-systolic (92%) and less likely mid-systolic (*i.e.*, within the second 50% of systolic ejection) (1%). Among patients with subsegmental PE, systolic notching was predominantly mid-systolic (19%) and less likely early-systolic (2%).

3.8.3. How to assess

1. Obtain a PSAX or SX short-axis view at the level of the aortic valve (*i.e.*, the base of the heart) such that the RVOT, pulmonic valve, and pulmonary artery are visualized.
2. Place the pulsed wave Doppler sampling gate in the RVOT approximately 0.5 cm proximal to the pulmonary valve (Fig. 9), with the beam aligned roughly in the direction of blood flow.
3. By pressing the pulsed wave Doppler button again, the pulmonary artery systolic ejection waveform appears as a downward deflection on the y-axis.
4. The waveform can be assessed qualitatively. The sweep speed of the study should be increased in order to stretch out the waveform for better discrimination of time intervals.
   a. Early-systolic notching refers to a sudden, transient decrease in velocity during the first half of the pulmonary arterial systolic ejection period (Fig. 9b).
   b. Mid-systolic notching refers to a transient decrease in velocity during the second half of the pulmonary arterial systolic ejection period.

3.8.4. Pearls and pitfalls

If the sampling gate inadvertently captures the pulmonic valve, the pulmonic valve waveform could mimic the “spike and dome” pattern seen with early-systolic notching [31]. The sampling gate should thus be placed in the RVOT sufficiently far away (*i.e.*, 0.5 cm) from the pulmonic valve. In addition, while commonly seen in pulmonary hypertension, this echocardiographic finding has also been described in cases of idiopathic pulmonary artery dilation [100].

3.9. 60/60 sign

3.9.1. Description

The 60/60 sign refers to both a tricuspid regurgitation pressure gradient (TRPG) ≤60 mmHg (corresponding to TRV_{max} < 3.9 m/s) (Fig. 6) and a pulmonary artery acceleration time (PAAT) < 60 ms (Fig. 10) [96,99]. Both parameters suggest an acute (*versus* chronic) process. The TRPG (i.e. $\Delta P_{RV\text{-}RA}$) can be determined from the simplified Bernoulli equation (4 x TRV_{max}^2) (Section 3.5.3). In

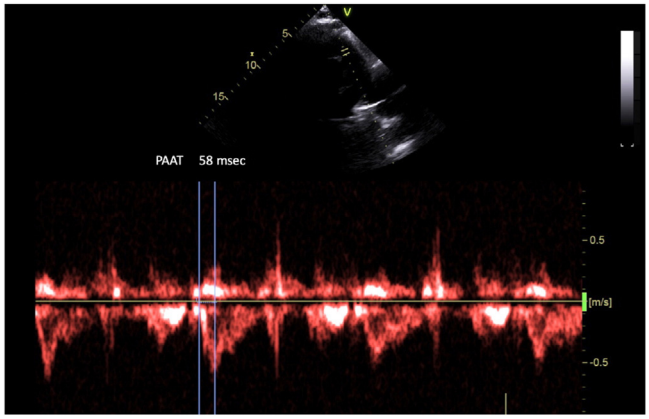

Fig. 10. Pulmonary artery acceleration time < 60 ms.

normotensive patients with acute PE, the TRPG has been found to have a mean of 33 mmHg [74]. In the setting of chronic pulmonary hypertension, the TRPG can reach > 60 mmHg (due to free wall hypertrophy) until there is eventually right ventricular failure [94,101].

PAAT refers to the time interval from the onset of pulmonary artery ejection to the peak flow velocity across the pulmonic valve in the right ventricular systolic ejection phase [101,102] (Fig. 9a). Normal range in adults is 136–153 ms [103]. PAAT has a weak correlation with age, body mass index, systolic and diastolic blood pressures, and diastolic heart function [102].

PAAT progressively shortens with increasing degrees of pulmonary pressure [9,42,93,102], with a strong correlation between PAAT and both TRV_{max} (r = 0.96) and PASP (r = 0.95) [42]. The diagnostic performance of PAAT is not affected by the etiology of pulmonary hypertension or by arrhythmias [101]. It is believed that the increased PVR and loss of lung compliance cause both a more rapid increase and a reduction of flow velocity [104]. This results in a more triangular-shaped (and lower-amplitude) Doppler profile, and thus a shorter PAAT [104]. Guidelines and studies denote a PAAT ≤ 105 ms as a cut-off for pulmonary hypertension [102,105,106]. An SRMA showed that PAAT is measurable in > 90% of patients [101].

In normal patients, a reflected pressure wave takes longer to return, and it hits the area of the pulmonic valve after the RV has completed its ejection [107]. In patients with chronic pulmonary arterial hypertension due to a distal etiology, PAAT is decreased but remains > 60 ms. The compliant pulmonary vasculature accepts the right ventricular output more gradually until the velocity peaks. In contrast, in patients with an acute proximal PE, PAAT will be < 60 ms. The less compliant pulmonary vasculature accepts the right ventricular output more quickly, resulting in an earlier velocity peak [94]. This occurs due to earlier return of the reflected pressure waves in the non-compliant pulmonary vessels [92].

Altogether, a short PAAT despite a moderate increase in TRPG (as in the 60/60 sign) may suggest the presence of proximal reflection points, such as PE [108]. In other words, the presence or absence of proximal PE (and not the level of pulmonary hypertension) may be the main determinant of the systolic flow velocity waveform [99].

3.9.2. Evidence

Studies have demonstrated 13–51% sensitivity and 69–98% specificity of the 60/60 sign for PE [20,31,96,99,109]. A single-center retrospective analysis of 511 consecutive patients with PE found that sensitivity was generally higher in patients with shock or hypotension [109]. Another retrospective study specifically showed that for sub-massive and massive PE, there was 51% sensitivity and 96% specificity, *versus* 7% sensitivity and 94% specificity for subsegmental PE [31]. Of patients without shock or hypotension, the 60/60 sign is much more sensitive when other echocardiographic parameters of right ventricular dysfunction are present (41.6% *versus* 5.9%) [109].

For PAAT itself, an SRMA showed 84% sensitivity and 84% specificity for prediction of pulmonary hypertension (PAP > 25 mmHg) [101]. Intraobserver variability has been shown to be 7.3 ± 6.7% with an interobserver variability of 8.8 ± 6.5% [106] and an interobserver reliability of 99.5% [104].

3.9.3. How to assess

To obtain TRPG:

1. Determine the TRV_{max} (Fig. 6) (Section 3.4.3).
2. Enter that value into the simplified Bernoulli equation: 4 x TRV_{max}^2 (Section 3.5.3).

To obtain PAAT:

1. Obtain the pulmonary artery systolic ejection velocity waveform (Section 3.8.3).
2. Use the cursor to measure the time interval from the onset of systolic pulmonary artery ejection to the velocity peak (Fig. 10a).

3.9.4. Pearls and pitfalls

From a clinical perspective, normal patients will also have a TRPG < 60 mmHg. Thus, the 60/60 sign should only be applied in patients being evaluated for PE. From a technical perspective, the same precaution previously described for proper sampling gate placement applies for obtaining the pulmonary artery systolic ejection waveform (see Section 3.8.4) [31]. However, very precise angulation of the pulsed wave Doppler beam is not necessary—the desired measurement is the time for the blood velocity to peak, not the amplitude of the velocity peak itself.

3.10. Speckle tracking demonstrating decreased right ventricular free wall strain

3.10.1. Description

An emerging trend in the evaluation for right ventricular strain is the use of speckle tracking. Sound waves emitted from the transducer are reflected due to relative differences in acoustic impedance between different areas of the myocardium. Dedicated software measures the scatter reflections, interprets these unique myocardial speckles as gray-scale spots, and tracks their frame-by-frame movement in any direction within the imaging plane (Video 6) [9,110–113]. This offline process is applied to previously saved video clips in order to generate two-dimensional strain curves for the right ventricular free wall (Fig. 11). Right ventricular strain refers to the percentage change in myocardial deformation (*i.e.*, in the length of a myocardial segment) [9]. It correlates closely with RVEF by MRI, sonomicrometry, and radionucleotide studies [114–118]. In the context of suspected or diagnosed PE, longitudinal strain (*i.e.*, the predominant right ventricular contractile pattern) refers to the percentage of free wall systolic shortening from base to apex [10].

Different ultrasound machines and vendors utilize unique platforms, leading to varied quantitative parameters for what is considered normal [9]. There has been a concerted effort by a joint ASE-EACVI Task Force to encourage inter-vendor standardization for the algorithms and parameters for strain [119]. Currently, the ASE and EACVI posit a mean percentage of right ventricular free wall strain as -29% ± 4.5%, with an abnormality threshold being > −20% (or < 20% in magnitude) [10].

3.10.2. Evidence

Both global longitudinal strain and strain of individual right ventricular segments are reduced in patients with PE [76,110,120–124]. Studies have also demonstrated lesser strain in the mid-right ventricular free wall as compared to the basal and apical segments, in a pattern similar to McConnell's sign [125,126]. This strain analysis pattern in patients with PE has been associated with in-hospital adverse events (*e.g.*, PE-related death, need for additive treatments such as thrombolysis or pulmonary artery thromboembolectomy, eed of inotropes due to unstable vital signs, and PE-related death), 30-day mortality, and 6-month mortality [76,127,128]. Strain of the mid-free wall can thus help differentiate the intermediate and high-risk patients from the low-risk patients with PE, which in turn may guide management [76,122,124,128]. Interventions that lead to hemodynamic improvement are usually accompanied by improvement in strain [129].

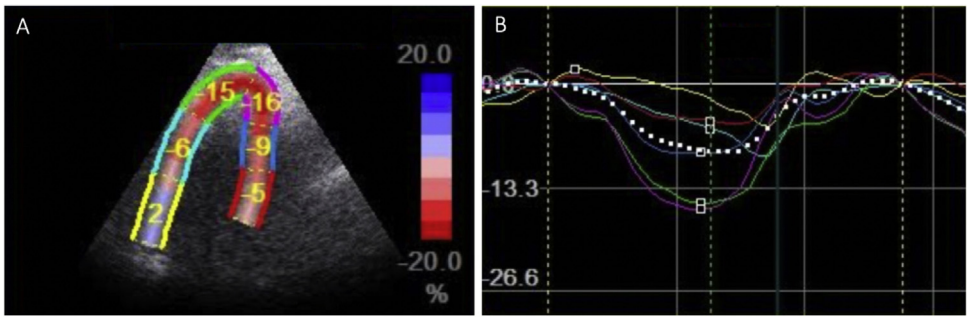

Fig. 11. Speckle-tracking evaluation of right ventricular free wall strain: a) Software analysis generates strain values for the three myocardial segments (basal, mid-free wall, apex) of the right ventricular free wall. Note how the mid-free wall strain is lower in magnitude compared to the apex, in a pattern analogous to McConnell's sign. Though the septal segments are captured in this image, they are not generally considered for the assessment of right ventricular dysfunction. b) Generation of strain curves corresponding to the individual myocardial segments (image courtesy of Robert R. Ehrman MD).

3.10.3. How to assess

1) Acquire a high-quality RV-focused A4C view.
   a) To achieve the optimal frame rate, adjust the depth to the minimum required such that the RV occupies most of the image sector.
      i) The ASE and European Association of Echocardiography recommend 40–80 frames per second.
         (1) In tachycardia, higher frame rates are recommended to avoid undersampling.
      ii) At lower-than-optimal frame rates, a large displacement of speckles between successive frames precludes satisfactory tracking of those speckles.
      iii) At higher-than-optimal frame rates, with fewer ultrasound beams in each frame, spatial resolution will be compromised.
2) Save a video containing at least 3 consecutive cardiac cycles.
   a) At least one complete cardiac cycle (*i.e.*, the middle one) without truncation will thus be available for offline analysis.
   b) The patient should hold a shallow breath during video acquisition to avoid shifting of the heart in the chest due to respiration.
3) Within the speckle-tracking program, delineate the free wall endocardial border at end-diastole so that the software can define the region of interest (*i.e.*, the entire myocardial thickness, while excluding the pericardium). Adjust manually as needed.
4) Allow the software to track the myocardial speckles frame-by-frame in the video clip (Video 6).
5) Once the tracking is approved by the user, the software will produce strain values (Fig. 11a) and corresponding strain curves (Fig. 11b).

3.10.4. Pearls and pitfalls

From a clinical perspective, whereas some echocardiographic parameters of right ventricular strain only manifest in intermediate and high-risk patients, one advantage of speckle tracking is that even smaller derangements in strain may offer diagnostic and prognostic value across the spectrum of disease. From a technical perspective, an advantage is that its measurements are angle-independent within the acquired imaging plane (however, since axial resolution is superior to lateral resolution, longitudinal strain parallel to the ultrasound beam has the best accuracy) [130]. In addition, the software provides simultaneous sampling from multiple sites of the myocardial wall. As a result, speckle tracking allows evaluation of longitudinal, circumferential, and radial strain within the same heartbeat.

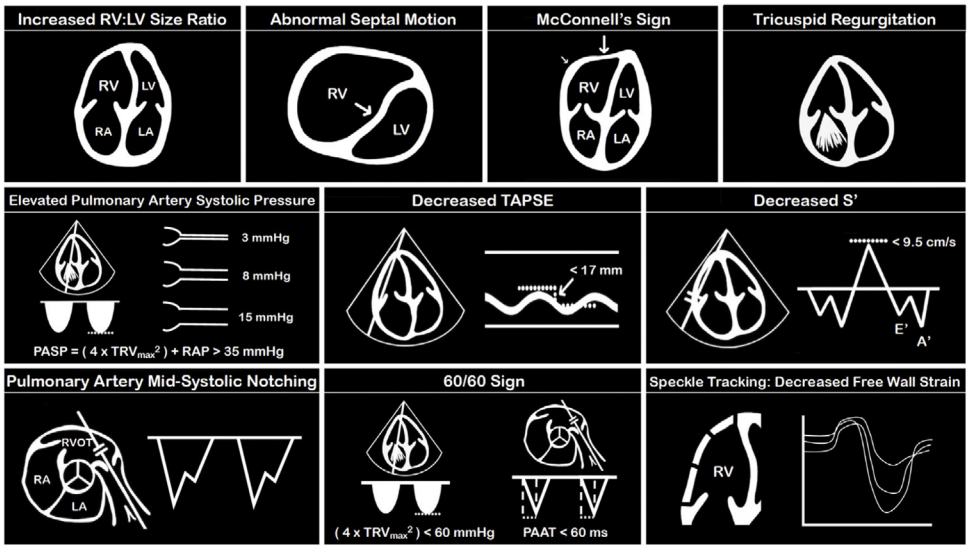

Fig. 12. Summary infographic for using POCUS to evaluate for acute right ventricular strain (designed by Linda Qiu MD for this manuscript).

The major disadvantage is the inter-vendor variability in algorithms that produces non-standardized parameters for normal and abnormal values of strain. Additionally, the ability to perform speckle-tracking analysis is dependent on high-quality images. Other limitations are that global assessments for strain are determined from a single cardiac view, and regional velocities may not represent global right ventricular function [9]. However, while global longitudinal strain from the A4C view measures only the lateral free wall, one study found no significant differences in strain when evaluating the apical 2- and 3-chamber views of the RV as well [131]. Lastly, speckle tracking cannot distinguish between active and passive deformation [110].

4. Conclusion

The POCUS evaluation for acute right ventricular strain is a critical tool for physicians in evaluating patients with suspected PE (Fig. 12). The most commonly performed and easily recognized qualitative findings are increased RV:LV size ratio and abnormal septal motion. Appearance of McConnell's sign and TR can increase the diagnostic likelihood when other findings are present. Quantitative estimation of the PASP using the TR Doppler technique can point to either an acute or chronic elevation, as well as suggested by another diagnosis when pulmonary artery pressures are normal. TAPSE and (to a lesser extent) S' represent easily performed and repeatable quantitative parameters for assessment of right ventricular longitudinal contraction. Determination of acuity can also be achieved by examining the pulmonary artery systolic ejection waveform—through both the presence of pulmonary artery early/mid-systolic notching and measurement of the PAAT for the 60/60 sign. Lastly, speckle tracking represents an offline software analysis that evaluates right ventricular free wall strain through the frame-by-frame tracking of individual myocardial speckles. Understanding these echocardiographic findings–while appreciating their limitations–can assist physicians to better assess for acute right ventricular strain at the patient's bedside.

Informed consent and patient details

The authors declare that this report does not contain any personal information that could lead to the identification of the patient(s).

Disclosure of interest

The authors have no competing interest to declare.

Funding

None.

Author contributions

All authors (SA, TS, MG) contributed to the literature search, writing of the manuscript, and its review prior to submission. Stephen Alerhand, Tina Sundaram, Michael Gottlieb: Conceptualization, Writing – Original Draft, Writing – Review & Editing.

Acknowledgements

The authors wish to thank Robert Ehrman MD for reviewing Section 3.10 on speckle tracking and contributing the accompanying Video 6 and Fig. 11, as well as Linda Qiu MD for her design of the summary infographic in Fig. 12.

Appendix A. Supplementary data

Supplementary material related to this article can be found, in the online version, at doi:https://doi.org/10.1016/j.accpm.2021.100852.

References

[1] Torbicki A, Perrier A, Konstantinides S, Agnelli G, Galie N, Pruszczyk P, et al. Guidelines on the diagnosis and management of acute pulmonary embolism: the Task Force for the Diagnosis and Management of Acute Pulmonary Embolism of the European Society of Cardiology (ESC). Eur Heart J 2008;29(18):2276–315.
[2] Roy PM, Meyer G, Vielle B, Le Gall C, Verschuren F, Carpentier F, et al. Appropriateness of diagnostic management and outcomes of suspected pulmonary embolism. Ann Intern Med 2006;144(3):157–64.
[3] Dwyer KH, Rempell JS, Stone MB. Diagnosing centrally located pulmonary embolisms in the emergency department using point-of-care ultrasound. Am J Emerg Med 2018;36(7):1145–50.
[4] Daley JI, Dwyer KH, Grunwald Z, Shaw DL, Stone MB, Schick A, et al. Increased sensitivity of focused cardiac ultrasound for pulmonary embolism in emergency department patients with abnormal vital signs. Acad Emerg Med 2019;26(11):1211–20.
[5] Grifoni S, Olivotto I, Cecchini P, Pieralli F, Camaiti A, Santoro G, et al. Short-term clinical outcome of patients with acute pulmonary embolism, normal blood pressure, and echocardiographic right ventricular dysfunction. Circulation 2000;101(24):2817–22.
[6] Kasper W, Konstantinides S, Geibel A, Tiede N, Krause T, Just H. Prognostic significance of right ventricular afterload stress detected by echocardiography in patients with clinically suspected pulmonary embolism. Heart 1997;77(4):346–9.
[7] Ribeiro A, Lindmarker P, Juhlin-Dannfelt A, Johnsson H, Jorfeldt L. Echocardiography Doppler in pulmonary embolism: right ventricular dysfunction as a predictor of mortality rate. Am Heart J 1997;134(3):479–87.
[8] Scridon T, Scridon C, Skali H, Alvarez A, Goldhaber SZ, Solomon SD. Prognostic significance of troponin elevation and right ventricular enlargement in acute pulmonary embolism. Am J Cardiol 2005;96(2):303–5.
[9] Rudski LG, Lai WW, Afilalo J, Hua L, Handschumacher MD, Chandrasekaran K, et al. Guidelines for the echocardiographic assessment of the right heart in adults: a report from the American Society of Echocardiography endorsed by the European Association of Echocardiography, a registered branch of the European Society of Cardiology, and the Canadian Society of Echocardiography. J Am Soc Echocardiogr 2010;23(7):685–713. quiz 86–88.
[10] Lang RM, Badano LP, Mor-Avi V, Afilalo J, Armstrong A, Ernande L, et al. Recommendations for cardiac chamber quantification by echocardiography in adults: an update from the American Society of Echocardiography and the European Association of Cardiovascular Imaging. J Am Soc Echocardiogr 2015;28(1):1–39. e14.
[11] Fields JM, Davis J, Girson L, Au A, Potts J, Morgan CJ, et al. Transthoracic echocardiography for diagnosing pulmonary embolism: a systematic review and meta-analysis. J Am Soc Echocardiogr 2017;30(7):714–23. e4.
[12] Dresden S, Mitchell P, Rahimi L, Leo M, Rubin-Smith J, Bibi S, et al. Right ventricular dilatation on bedside echocardiography performed by emergency physicians aids in the diagnosis of pulmonary embolism. Ann Emerg Med 2014;63(1):16–24.
[13] Ling LF, Obuchowski NA, Rodriguez L, Popovic Z, Kwon D, Marwick TH. Accuracy and interobserver concordance of echocardiographic assessment of right ventricular size and systolic function: a quality control exercise. J Am Soc Echocardiogr 2012;25(7):709–13.
[14] Ho SY, Nihoyannopoulos P. Anatomy, echocardiography, and normal right ventricular dimensions. Heart 2006;92 Suppl 1:i2–13.
[15] Foale R, Nihoyannopoulos P, McKenna W, Kleinebenne A, Nadazdin A, Rowland E, et al. Echocardiographic measurement of the normal adult right ventricle. Br Heart J 1986;56(1):33–44.
[16] Bova C, Greco F, Misuraca G, Serafini O, Crocco F, Greco A, et al. Diagnostic utility of echocardiography in patients with suspected pulmonary embolism. Am J Emerg Med 2003;21(3):180–3.
[17] Grifoni S, Olivotto I, Cecchini P, Pieralli F, Camaiti A, Santoro G, et al. Utility of an integrated clinical, echocardiographic, and venous ultrasonographic approach for triage of patients with suspected pulmonary embolism. Am J Cardiol 1998;82(10):1230–5.
[18] Jackson RE, Rudoni RR, Hauser AM, Pascual RG, Hussey ME. Prospective evaluation of two-dimensional transthoracic echocardiography in emergency department patients with suspected pulmonary embolism. Acad Emerg Med 2000;7(9):994–8.
[19] Jardin F, Dubourg O, Gueret P, Delorme G, Bourdarias JP. Quantitative two-dimensional echocardiography in massive pulmonary embolism: emphasis on ventricular interdependence and leftward septal displacement. J Am Coll Cardiol 1987;10(6):1201–6.
[20] Lodato JA, Ward RP, Lang RM. Echocardiographic predictors of pulmonary embolism in patients referred for helical CT. Echocardiography 2008;25(6):584–90.
[21] Rodrigues AC, Cordovil A, Monaco C, Guimaraes L, Cury A, Naccarato GA, et al. Right ventricular assessment by tissue-Doppler echocardiography in acute pulmonary embolism. Arq Bras Cardiol 2013;100(6):524–30.
[22] Rudoni RR, Jackson RE, Godfrey GW, Bonfiglio AX, Hussey ME, Hauser AM. Use of two-dimensional echocardiography for the diagnosis of pulmonary embolus. J Emerg Med 1998;16(1):5–8.
[23] Samaranayake CB, Royle G, Jackson S, Yap E. Right ventricular dysfunction and pulmonary hypertension following sub-massive pulmonary embolism. Clin Respir J 2017;11(6):867–74.

[24] Vieillard-Baron A. Assessment of right ventricular function. Curr Opin Crit Care 2009;15(3):254–60.
[25] Mori S, Nakatani S, Kanzaki H, Yamagata K, Take Y, Matsuura Y, et al. Patterns of the interventricular septal motion can predict conditions of patients with pulmonary hypertension. J Am Soc Echocardiogr 2008;21(4):386–93.
[26] Vardan S, Mookherjee S, Smulyan HS, Obeid AI. Echocardiography in pulmonary embolism. Jpn Heart J 1983;24(1):67–78.
[27] McConnell MV, Solomon SD, Rayan ME, Come PC, Goldhaber SZ, Lee RT. Regional right ventricular dysfunction detected by echocardiography in acute pulmonary embolism. Am J Cardiol 1996;78(4):469–73.
[28] Calvin Jr JE. Pressure segment length analysis of right ventricular function: influence of loading conditions. Am J Physiol 1991;260(4 Pt 2):H1087–97.
[29] Janz RF, Kubert BR, Pate EF, Moriarty TF. Effect of shape on pressure-volume relationships of ellipsoidal shells. Am J Physiol 1980;238(6):H917–26.
[30] Come PC. Echocardiographic recognition of pulmonary arterial disease and determination of its cause. Am J Med 1988;84(3 Pt 1):384–94.
[31] Afonso L, Sood A, Akintoye E, Gorcsan 3rd J, Rehman MU, Kumar K, et al. A Doppler echocardiographic pulmonary flow marker of massive or submassive acute pulmonary embolus. J Am Soc Echocardiogr 2019;32(7):799–806.
[32] Casazza F, Bongarzoni A, Capozi A, Agostoni O. Regional right ventricular dysfunction in acute pulmonary embolism and right ventricular infarction. Eur J Echocardiogr 2005;6(1):11–4.
[33] Tuzovic M, Adigopula S, Amsallem M, Kobayashi Y, Kadoch M, Boulate D, et al. Regional right ventricular dysfunction in acute pulmonary embolism: relationship with clot burden and biomarker profile. Int J Cardiovasc Imaging 2016;32(3):389–98.
[34] Kopecna D, Briongos S, Castillo H, Moreno C, Recio M, Navas P, et al. Interobserver reliability of echocardiography for prognostication of normotensive patients with pulmonary embolism. Cardiovasc Ultrasound 2014;12:29.
[35] Shah P, Schleifer JW, Mookadam F, Chandrasekaran K. Right ventricular myocardial infarction: an underrecognized aetiology of McConnell's sign. Eur Heart J Cardiovasc Imaging 2015;16(2):225.
[36] Longo SA, Echegaray A, Acosta CM, Rinaldi LI, Cabrera Schulmeyer MC, Olavide Goya I. McConnell's sign in intra-operative acute right ventricle ischaemia: an under-recognized aetiology. Rev Esp Anestesiol Reanim 2016;63(9):528–32.
[37] Badesch DB, Champion HC, Sanchez MA, Hoeper MM, Loyd JE, Manes A, et al. Diagnosis and assessment of pulmonary arterial hypertension. J Am Coll Cardiol 2009;54(1 Suppl.):S55–66.
[38] Task Force for D, Treatment of Pulmonary Hypertension of European Society of C, European Respiratory S, International Society of H, Lung T, Galie N, et al. Guidelines for the diagnosis and treatment of pulmonary hypertension. Eur Respir J 2009;34(6):1219–63.
[39] Lau EM, Manes A, Celermajer DS, Galie N. Early detection of pulmonary vascular disease in pulmonary arterial hypertension: time to move forward. Eur Heart J 2011;32(20):2489–98.
[40] McQuillan BM, Picard MH, Leavitt M, Weyman AE. Clinical correlates and reference intervals for pulmonary artery systolic pressure among echocardiographically normal subjects. Circulation 2001;104(23):2797–802.
[41] Mutlak D, Aronson D, Lessick J, Reisner SA, Dabbah S, Agmon Y. Functional tricuspid regurgitation in patients with pulmonary hypertension: is pulmonary artery pressure the only determinant of regurgitation severity? Chest 2009;135(1):115–21.
[42] Yared K, Noseworthy P, Weyman AE, McCabe E, Picard MH, Baggish AL. Pulmonary artery acceleration time provides an accurate estimate of systolic pulmonary arterial pressure during transthoracic echocardiography. J Am Soc Echocardiogr 2011;24(6):687–92.
[43] Borgeson DD, Seward JB, Miller Jr FA, Oh JK, Tajik AJ. Frequency of Doppler measurable pulmonary artery pressures. J Am Soc Echocardiogr 1996;9(6):832–7.
[44] Aduen JF, Castello R, Lozano MM, Hepler GN, Keller CA, Alvarez F, et al. An alternative echocardiographic method to estimate mean pulmonary artery pressure: diagnostic and clinical implications. J Am Soc Echocardiogr 2009;22(7):814–9.
[45] Berger M, Haimowitz A, Van Tosh A, Berdoff RL, Goldberg E. Quantitative assessment of pulmonary hypertension in patients with tricuspid regurgitation using continuous wave Doppler ultrasound. J Am Coll Cardiol 1985;6(2):359–65.
[46] Aessopos A, Farmakis D, Taktikou H, Loukopoulos D. Doppler-determined peak systolic tricuspid pressure gradient in persons with normal pulmonary function and tricuspid regurgitation. J Am Soc Echocardiogr 2000;13(7):645–9.
[47] Moreno FL, Hagan AD, Holmen JR, Pryor TA, Strickland RD, Castle CH. Evaluation of size and dynamics of the inferior vena cava as an index of right-sided cardiac function. Am J Cardiol 1984;53(4):579–85.
[48] Ciozda W, Kedan I, Kehl DW, Zimmer R, Khandwalla R, Kimchi A. The efficacy of sonographic measurement of inferior vena cava diameter as an estimate of central venous pressure. Cardiovasc Ultrasound 2016;14(1):33.
[49] Brennan JM, Blair JE, Goonewardena S, Ronan A, Shah D, Vasaiwala S, et al. Reappraisal of the use of inferior vena cava for estimating right atrial pressure. J Am Soc Echocardiogr 2007;20(7):857–61.
[50] Bendjelid K, Romand JA, Walder B, Suter PM, Fournier G. Correlation between measured inferior vena cava diameter and right atrial pressure depends on the echocardiographic method used in patients who are mechanically ventilated. J Am Soc Echocardiogr 2002;15(9):944–9.
[51] Mitaka C, Nagura T, Sakanishi N, Tsunoda Y, Amaha K. Two-dimensional echocardiographic evaluation of inferior vena cava, right ventricle, and left ventricle during positive-pressure ventilation with varying levels of positive end-expiratory pressure. Crit Care Med 1989;17(3):205–10.
[52] Jue J, Chung W, Schiller NB. Does inferior vena cava size predict right atrial pressures in patients receiving mechanical ventilation? J Am Soc Echocardiogr 1992;5(6):613–9.
[53] Finnerty NM, Panchal AR, Boulger C, Vira A, Bischof JJ, Amick C, et al. Inferior vena cava measurement with ultrasound: what is the best view and best mode? West J Emerg Med 2017;18(3):496–501.
[54] Fields JM, Lee PA, Jenq KY, Mark DG, Panebianco NL, Dean AJ. The interrater reliability of inferior vena cava ultrasound by bedside clinician sonographers in emergency department patients. Acad Emerg Med 2011;18(1):98–101.
[55] Akkaya A, Yesilaras M, Aksay E, Sever M, Atilla OD. The interrater reliability of ultrasound imaging of the inferior vena cava performed by emergency residents. Am J Emerg Med 2013;31(10):1509–11.
[56] Zhou AZ, Green RS, Haines EJ, Vazquez MN, Tay ET, Tsung JW. Interobserver agreement of inferior vena cava ultrasound collapse duration and correlated outcomes in children with dehydration. Pediatr Emerg Care 2020. http://dx.doi.org/10.1097/PEC.0000000000002150. Online ahead of print.
[57] Lang RM, Bierig M, Devereux RB, Flachskampf FA, Foster E, Pellikka PA, et al. Recommendations for chamber quantification: a report from the american society of echocardiography's guidelines and standards committee and the chamber quantification writing group, developed in conjunction with the european association of echocardiography, a branch of the European society of cardiology. J Am Soc Echocardiogr 2005;18(12):1440–63.
[58] Milan A, Magnino C, Veglio F. Echocardiographic indexes for the non-invasive evaluation of pulmonary hemodynamics. J Am Soc Echocardiogr 2010;23(3):225–39. quiz 332–334.
[59] Ommen SR, Nishimura RA, Hurrell DG, Klarich KW. Assessment of right atrial pressure with 2-dimensional and Doppler echocardiography: a simultaneous catheterization and echocardiographic study. Mayo Clin Proc 2000;75(1):24–9.
[60] Nakao S, Come PC, McKay RG, Ransil BJ. Effects of positional changes on inferior vena caval size and dynamics and correlations with right-sided cardiac pressure. Am J Cardiol 1987;59(1):125–32.
[61] Fisher MR, Forfia PR, Chamera E, Housten-Harris T, Champion HC, Girgis RE, et al. Accuracy of Doppler echocardiography in the hemodynamic assessment of pulmonary hypertension. Am J Respir Crit Care Med 2009;179(7):615–21.
[62] Dahhan T, Alenezi F, Samad Z, Rajagopal S. Echocardiography in the risk assessment of acute pulmonary embolism. Semin Respir Crit Care Med 2017;38(1):18–28.
[63] Bystrom B, Lindqvist P, Henein M. The right ventricle: knowing what is right. Int J Cardiovasc Imaging 2008;24(7):701–2.
[64] Alerhand S, Hickey SM. Tricuspid annular plane systolic excursion (TAPSE) for risk stratification and prognostication of patients with pulmonary embolism. J Emerg Med 2020;58(3):449–56.
[65] Carlsson M, Ugander M, Heiberg E, Arheden H. The quantitative relationship between longitudinal and radial function in left, right, and total heart pumping in humans. Am J Physiol Heart Circ Physiol 2007;293(1):H636–44.
[66] Ueti OM, Camargo EE, Ueti Ade A, de Lima-Filho EC, Nogueira EA. Assessment of right ventricular function with Doppler echocardiographic indices derived from tricuspid annular motion: comparison with radionuclide angiography. Heart 2002;88(3):244–8.
[67] Park JR, Chang SA, Jang SY, No HJ, Park SJ, Choi SH, et al. Evaluation of right ventricular dysfunction and prediction of clinical outcomes in acute pulmonary embolism by chest computed tomography: comparisons with echocardiography. Int J Cardiovasc Imaging 2012;28(4):979–87.
[68] Kjaergaard J, Petersen CL, Kjaer A, Schaadt BK, Oh JK, Hassager C. Evaluation of right ventricular volume and function by 2D and 3D echocardiography compared to MRI. Eur J Echocardiogr 2006;7(6):430–8.
[69] Kaul S, Tei C, Hopkins JM, Shah PM. Assessment of right ventricular function using two-dimensional echocardiography. Am Heart J 1984;107(3):526–31.
[70] Miller D, Farah MG, Liner A, Fox K, Schluchter M, Hoit BD. The relation between quantitative right ventricular ejection fraction and indices of tricuspid annular motion and myocardial performance. J Am Soc Echocardiogr 2004;17(5):443–7.
[71] Pruszczyk P, Goliszek S, Lichodziejewska B, Kostrubiec M, Ciurzynski M, Kurnicka K, et al. Prognostic value of echocardiography in normotensive patients with acute pulmonary embolism. JACC Cardiovasc Imaging 2014;7(6):553–60.
[72] Lobo JL, Holley A, Tapson V, Moores L, Oribe M, Barron M, et al. Prognostic significance of tricuspid annular displacement in normotensive patients with acute symptomatic pulmonary embolism. J Thromb Haemost 2014;12(7):1020–7.
[73] Paczynska M, Sobieraj P, Burzynski L, Kostrubiec M, Wisniewska M, Bienias P, et al. Tricuspid annulus plane systolic excursion (TAPSE) has superior predictive value compared to right ventricular to left ventricular ratio in normotensive patients with acute pulmonary embolism. Arch Med Sci 2016;12(5):1008–14.
[74] Ciurzynski M, Kurnicka K, Lichodziejewska B, Kozlowska M, Plywaczewska M, Sobieraj P, et al. Tricuspid regurgitation peak gradient (TRPG)/Tricuspid annulus plane systolic excursion (TAPSE)- a novel parameter for stepwise echocardiographic risk stratification in normotensive patients with acute pulmonary embolism. Circ J 2018;82(4):1179–85.

[75] Rydman R, Soderberg M, Larsen F, Caidahl K, Alam M. Echocardiographic evaluation of right ventricular function in patients with acute pulmonary embolism: a study using tricuspid annular motion. Echocardiography 2010;27(3):286–93.
[76] Vitarelli A, Barilla F, Capotosto L, D'Angeli I, Truscelli G, De Maio M, et al. Right ventricular function in acute pulmonary embolism: a combined assessment by three-dimensional and speckle-tracking echocardiography. J Am Soc Echocardiogr 2014;27(3):329–38.
[77] Daley J, Grotberg J, Pare J, Medoro A, Liu R, Hall MK, et al. Emergency physician performed tricuspid annular plane systolic excursion in the evaluation of suspected pulmonary embolism. Am J Emerg Med 2017;35(1):106–11.
[78] Sade LE, Gulmez O, Ozyer U, Ozgul E, Agildere M, Muderrisoglu H. Tissue Doppler study of the right ventricle with a multisegmental approach: comparison with cardiac magnetic resonance imaging. J Am Soc Echocardiogr 2009;22(4):361–8.
[79] Tuller D, Steiner M, Wahl A, Kabok M, Seiler C. Systolic right ventricular function assessment by pulsed wave tissue Doppler imaging of the tricuspid annulus. Swiss Med Wkly 2005;135(31–32):461–8.
[80] Pavlicek M, Wahl A, Rutz T, de Marchi SF, Hille R, Wustmann K, et al. Right ventricular systolic function assessment: rank of echocardiographic methods vs. cardiac magnetic resonance imaging. Eur J Echocardiogr 2011;12(11):871–80.
[81] Wahl A, Praz F, Schwerzmann M, Bonel H, Koestner SC, Hullin R, et al. Assessment of right ventricular systolic function: comparison between cardiac magnetic resonance derived ejection fraction and pulsed-wave tissue Doppler imaging of the tricuspid annulus. Int J Cardiol 2011;151(1):58–62.
[82] Meluzin J, Spinarova L, Bakala J, Toman J, Krejci J, Hude P, et al. Pulsed Doppler tissue imaging of the velocity of tricuspid annular systolic motion; a new, rapid, and non-invasive method of evaluating right ventricular systolic function. Eur Heart J 2001;22(4):340–8.
[83] Gondi S, Dokainish H. Right ventricular tissue Doppler and strain imaging: ready for clinical use? Echocardiography 2007;24(5):522–32.
[84] Alam M, Wardell J, Andersson E, Samad BA, Nordlander R. Characteristics of mitral and tricuspid annular velocities determined by pulsed wave Doppler tissue imaging in healthy subjects. J Am Soc Echocardiogr 1999;12(8):618–28.
[85] Lindqvist P, Waldenstrom A, Henein M, Morner S, Kazzam E. Regional and global right ventricular function in healthy individuals aged 20-90 years: a pulsed Doppler tissue imaging study: Umea General Population Heart Study. Echocardiography 2005;22(4):305–14.
[86] Sutherland GR, Di Salvo G, Claus P, D'Hooge J, Bijnens B. Strain and strain rate imaging: a new clinical approach to quantifying regional myocardial function. J Am Soc Echocardiogr 2004;17(7):788–802.
[87] Vinereanu D, Khokhar A, Fraser AG. Reproducibility of pulsed wave tissue Doppler echocardiography. J Am Soc Echocardiogr 1999;12(6):492–9.
[88] Weyman AE, Dillon JC, Feigenbaum H, Chang S. Echocardiographic patterns of pulmonic valve motion with pulmonary hypertension. Circulation 1974;50(5):905–10.
[89] Tahara M, Tanaka H, Nakao S, Yoshimura H, Sakurai S, Tei C, et al. Hemodynamic determinants of pulmonary valve motion during systole in experimental pulmonary hypertension. Circulation 1981;64(6):1249–55.
[90] Kitabatake A, Inoue M, Asao M, Masuyama T, Tanouchi J, Morita T, et al. Noninvasive evaluation of pulmonary hypertension by a pulsed Doppler technique. Circulation 1983;68(2):302–9.
[91] Isobe M, Yazaki Y, Takaku F, Koizumi K, Hara K, Tsuneyoshi H, et al. Prediction of pulmonary arterial pressure in adults by pulsed Doppler echocardiography. Am J Cardiol 1986;57(4):316–21.
[92] Furuno Y, Nagamoto Y, Fujita M, Kaku T, Sakurai S, Kuroiwa A. Reflection as a cause of mid-systolic deceleration of pulmonary flow wave in dogs with acute pulmonary hypertension: comparison of pulmonary artery constriction with pulmonary embolisation. Cardiovasc Res 1991;25(2):118–24.
[93] Matsuda M, Sekiguchi T, Sugishita Y, Kuwako K, Iida K, Ito I. Reliability of noninvasive estimates of pulmonary hypertension by pulsed Doppler echocardiography. Br Heart J 1986;56(2):158–64.
[94] Torbicki A, Tramarin R, Morpurgo M. Role of echo/Doppler in the diagnosis of pulmonary embolism. Clin Cardiol 1992;15(11):805–10.
[95] Arkles JS, Opotowsky AR, Ojeda J, Rogers F, Liu T, Prassana V, et al. Shape of the right ventricular Doppler envelope predicts hemodynamics and right heart function in pulmonary hypertension. Am J Respir Crit Care Med 2011;183(2):268–76.
[96] Kurzyna M, Torbicki A, Pruszczyk P, Burakowska B, Fijalkowska A, Kober J, et al. Disturbed right ventricular ejection pattern as a new Doppler echocardiographic sign of acute pulmonary embolism. Am J Cardiol 2002;90(5):507–11.
[97] Torbicki A, Skwarski K, Hawrylkiewicz I, Pasierski T, Miskiewicz Z, Zielinski J. Attempts at measuring pulmonary arterial pressure by means of Doppler echocardiography in patients with chronic lung disease. Eur Respir J 1989;2(9):856–60.
[98] Takahama H, McCully RB, Frantz RP, Kane GC. Unraveling the RV ejection Doppler envelope: insight into pulmonary artery hemodynamics and disease severity. JACC Cardiovasc Imaging 2017;10(10 Pt B):1268–77.
[99] Torbicki A, Kurzyna M, Ciurzynski M, Pruszczyk P, Pacho R, Kuch-Wocial A, et al. Proximal pulmonary emboli modify right ventricular ejection pattern. Eur Respir J 1999;13(3):616–21.
[100] Bauman W, Wann LS, Childress R, Weyman AE, Feigenbaum H, Dillon J. Mid systolic notching of the pulmonary valve in the absence of pulmonary hypertension. Am J Cardiol 1979;43(5):1049–52.
[101] Wang YC, Huang CH, Tu YK. Pulmonary hypertension and pulmonary artery acceleration time: a systematic review and meta-analysis. J Am Soc Echocardiogr 2018;31(2):201–10. e3.
[102] Marra AM, Benjamin N, Ferrara F, Vriz O, D'Alto M, D'Andrea A, et al. Reference ranges and determinants of right ventricle outflow tract acceleration time in healthy adults by two-dimensional echocardiography. Int J Cardiovasc Imaging 2017;33(2):219–26.
[103] Tossavainen E, Soderberg S, Gronlund C, Gonzalez M, Henein MY, Lindqvist P. Pulmonary artery acceleration time in identifying pulmonary hypertension patients with raised pulmonary vascular resistance. Eur Heart J Cardiovasc Imaging 2013;14(9):890–7.
[104] Koestenberger M, Grangl G, Avian A, Gamillscheg A, Grillitsch M, Cvirn G, et al. Normal reference values and z scores of the pulmonary artery acceleration time in children and its importance for the assessment of pulmonary hypertension. Circ Cardiovasc Imaging 2017;10(1).
[105] Galie N, Humbert M, Vachiery JL, Gibbs S, Lang I, Torbicki A, et al. 2015 ESC/ERS Guidelines for the diagnosis and treatment of pulmonary hypertension: the Joint Task Force for the Diagnosis and Treatment of Pulmonary Hypertension of the European Society of Cardiology (ESC) and the European Respiratory Society (ERS): Endorsed by: Association for European Paediatric and Congenital Cardiology (AEPC), International Society for Heart and Lung Transplantation (ISHLT). Eur Heart J 2016;37(1):67–119.
[106] Dabestani A, Mahan G, Gardin JM, Takenaka K, Burn C, Allfie A, et al. Evaluation of pulmonary artery pressure and resistance by pulsed Doppler echocardiography. Am J Cardiol 1987;59(6):662–8.
[107] Kussmaul WG, Noordergraaf A, Laskey WK. Right ventricular-pulmonary arterial interactions. Ann Biomed Eng 1992;20(1):63–80.
[108] Castelain V, Herve P, Lecarpentier Y, Duroux P, Simonneau G, Chemla D. Pulmonary artery pulse pressure and wave reflection in chronic pulmonary thromboembolism and primary pulmonary hypertension. J Am Coll Cardiol 2001;37(4):1085–92.
[109] Kurnicka K, Lichodziejewska B, Goliszek S, Dzikowska-Diduch O, Zdonczyk O, Kozlowska M, et al. Echocardiographic pattern of acute pulmonary embolism: analysis of 511 consecutive patients. J Am Soc Echocardiogr 2016;29(9):907–13.
[110] Mor-Avi V, Lang RM, Badano LP, Belohlavek M, Cardim NM, Derumeaux G, et al. Current and evolving echocardiographic techniques for the quantitative evaluation of cardiac mechanics: ASE/EAE consensus statement on methodology and indications endorsed by the Japanese Society of Echocardiography. Eur J Echocardiogr 2011;12(3):167–205.
[111] Leitman M, Lysyansky P, Sidenko S, Shir V, Peleg E, Binenbaum M, et al. Two-dimensional strain-a novel software for real-time quantitative echocardiographic assessment of myocardial function. J Am Soc Echocardiogr 2004;17(10):1021–9.
[112] Pirat B, Khoury DS, Hartley CJ, Tiller L, Rao L, Schulz DG, et al. A novel feature-tracking echocardiographic method for the quantitation of regional myocardial function: validation in an animal model of ischemia-reperfusion. J Am Coll Cardiol 2008;51(6):651–9.
[113] Bansal M, Kasliwal RR. How do I do it? Speckle-tracking echocardiography. Indian Heart J 2013;65(1):117–23.
[114] Leong DP, Grover S, Molaee P, Chakrabarty A, Shirazi M, Cheng YH, et al. Nonvolumetric echocardiographic indices of right ventricular systolic function: validation with cardiovascular magnetic resonance and relationship with functional capacity. Echocardiography 2012;29(4):455–63.
[115] Focardi M, Cameli M, Carbone SF, Massoni A, De Vito R, Lisi M, et al. Traditional and innovative echocardiographic parameters for the analysis of right ventricular performance in comparison with cardiac magnetic resonance. Eur Heart J Cardiovasc Imaging 2015;16(1):47–52.
[116] Lu KJ, Chen JX, Profitis K, Kearney LG, DeSilva D, Smith G, et al. Right ventricular global longitudinal strain is an independent predictor of right ventricular function: a multimodality study of cardiac magnetic resonance imaging, real time three-dimensional echocardiography and speckle tracking echocardiography. Echocardiography 2015;32(6):966–74.
[117] Jamal F, Bergerot C, Argaud L, Loufouat J, Ovize M. Longitudinal strain quantitates regional right ventricular contractile function. Am J Physiol Heart Circ Physiol 2003;285(6):H2842–7.
[118] Lah M, Quelch K, Deacon NJ, McKenzie IF, Hogarth PM. Identification of the mouse beta Fc gamma RII polymorphism by direct sequencing of amplified genomic DNA. Immunogenetics 1990;31(3):202–6.
[119] Voigt JU, Pedrizzetti G, Lysyansky P, Marwick TH, Houle H, Baumann R, et al. Definitions for a common standard for 2D speckle tracking echocardiography: consensus document of the EACVI/ASE/Industry Task Force to standardize deformation imaging. J Am Soc Echocardiogr 2015;28(2):183–93.
[120] Trivedi SJ, Terluk AD, Kritharides L, Chow V, Chia EM, Byth K, et al. Right ventricular speckle tracking strain echocardiography in patients with acute pulmonary embolism. Int J Cardiovasc Imaging 2020;36(5):865–72.
[121] Ramberg E, Olausson M, Jorgensen TB, Nepper ML, Bhardwaj P, Binko TS, et al. Right atrial and ventricular function evaluated with speckle tracking in patients with acute pulmonary embolism. Am J Emerg Med 2017;35(1):136–43.
[122] Platz E, Hassanein AH, Shah A, Goldhaber SZ, Solomon SD. Regional right ventricular strain pattern in patients with acute pulmonary embolism. Echocardiography 2012;29(4):464–70.

[123] Sugiura E, Dohi K, Onishi K, Takamura T, Tsuji A, Ota S, et al. Reversible right ventricular regional non-uniformity quantified by speckle-tracking strain imaging in patients with acute pulmonary thromboembolism. J Am Soc Echocardiogr 2009;22(12):1353–9.
[124] Descotes-Genon V, Chopard R, Morel M, Meneveau N, Schiele F, Bernard Y. Comparison of right ventricular systolic function in patients with low risk and intermediate-to-high risk pulmonary embolism: a two-dimensional strain imaging study. Echocardiography 2013;30(3):301–8.
[125] Kjaergaard J, Sogaard P, Hassager C. Right ventricular strain in pulmonary embolism by Doppler tissue echocardiography. J Am Soc Echocardiogr 2004;17(11):1210–2.
[126] Mazur ES, Mazur VV, Rabinovich RM, Myasnikov KS. Right ventricular longitudinal strain in acute pulmonary embolism and right ventricular myocardial infarction in patients with McConnell's sign. Kardiologiia 2020;60(7):20–7.
[127] Lee K, Kwon O, Lee EJ, Sin MJ, Lee JS, Lee S, et al. Prognostic value of echocardiographic parameters for right ventricular function in patients with acute non-massive pulmonary embolism. Heart Vessels 2019;34(7):1187–95.
[128] Dahhan T, Siddiqui I, Tapson VF, Velazquez EJ, Sun S, Davenport CA, et al. Clinical and echocardiographic predictors of mortality in acute pulmonary embolism. Cardiovasc Ultrasound 2016;14(1):44.
[129] Claus P, Omar AMS, Pedrizzetti G, Sengupta PP, Nagel E. Tissue tracking technology for assessing cardiac mechanics: principles, normal values, and clinical applications. JACC Cardiovasc Imaging 2015;8(12):1444–60.
[130] Pedrizzetti G, Claus P, Kilner PJ, Nagel E. Principles of cardiovascular magnetic resonance feature tracking and echocardiographic speckle tracking for informed clinical use. J Cardiovasc Magn Reson 2016;18(1):51.
[131] Rajagopal S, Forsha DE, Risum N, Hornik CP, Poms AD, Fortin TA, et al. Comprehensive assessment of right ventricular function in patients with pulmonary hypertension with global longitudinal peak systolic strain derived from multiple right ventricular views. J Am Soc Echocardiogr 2014;27(6):657–65. e3.